Associated conference: 5th International Small Sample Test Techniques Conference

Conference location: Swansea University, Bay Campus

Conference date: 10th - 12 July 2018

How to cite: Kamaya, M. 2018. Numerical Investigations of Small Punch Tests for Determining Tensile Properties. *Ubiquity Proceedings*, 1(S1): 27 DOI: https://doi.org/10.5334/uproc.27

Published on: 10 September 2018

Numerical Investigations of Small Punch Tests for Determining Tensile Properties

M. Kamaya [1]*

[1] Institute of Nuclear Safety System, Inc.
* Correspondence: kamaya@inss.co.jp; Tel.: +81-50-7105-0096

Abstract: Small punch tests were conducted for carbon steel specimens prepared with and without cold working. A digital image correlation technique was applied to measure displacement. Finite element analyses using the true stress-strain curves including post-necking strain could reproduce the load-displacement (LD) curve. Use of the nominal stress-strain curve obtained by the conventional tensile test was not enough to simulate the maximum load. It was found that the maximum load did not depend on the ultimate strength. Therefore, the ultimate strength prediction using the maximum load in the LD curve may not be valid for the general case. On the other hand, the yield strength correlated well with the deflection point in the LD curve. A new equation was proposed to estimate the yield strength that takes into consideration the influence of the specimen thickness.

Keywords: small punch test; yield strength, ultimate strength, tensile properties; finite element analysis

1. Introduction

The small punch (SP) test has been applied to estimate tensile properties such as the yield and ultimate strengths [1-3]. Since a tiny specimen is used for the SP test, it is possible to determine the tensile properties for a small piece taken from an actual component. The local properties of inhomogeneous materials such as welds also can be obtained by the SP test. The tensile properties are determined from the load-displacement (LD) curve, which consists of four regions [2]: the elastic bending, plastic bending, membrane stretching and failure regions. The LD curve exhibits linear (elastic) deformation at the beginning of the SP test, and then, deflects due to yielding. After yielding, the curve increases almost linearly and peaks before an abrupt load drop due to fracture of the specimen. The deformation of the specimen has been correlated to the stress-strain curve. The yield strength has been correlated to the initial deflection of the LD curve and the ultimate strength has been determined using the maximum load during the SP test [1,2].

Since the deformation of a specimen during the SP test is quite different from that of tensile tests, it is difficult to find a clear correlation between the LD curve and the stress-strain curve. Therefore, determination of the tensile properties from the LD curve has been rather empirical. Finite element analysis (FEA) for various conditions can be an effective tool to get a generalized and comprehensive correlation between the tensile properties and the LD curve. Although it is relatively easy to simulate the elastic and plastic bending regions, it is difficult to reproduce the peak of the LD curve by FEA [3,4]. Since the specimen deforms largely during the SP test, the stress-strain curve over the necking strain is required for precise simulation of the SP test.

In this study, SP tests were conducted for cold worked and non-cold worked carbon steel specimens. Then, FEAs were performed to simulate the tests using stress-strain curves obtained in a previous study [5], in which true stress-strain curves including post-necking strain were determined by an iterative process using FEAs and the local strain measurement technique. By performing FEAs for various conditions, influences of the stress-strain curve and specimen thickness on the determination of the yield and ultimate strengths were discussed.

2. Small punch tests

2.1. Material

The material used for the SP tests was carbon steel plate for welding structures (SM490A in JIS), whose alloying constituents (in wt%) were: C, 0.16; Si, 0.31; Mn, 1.35; P, 0.019; S, 0.004; and V, 0.033. A rolling process was applied to the plate to induce cold working at room temperature. The degree of cold working was quantified from the nominal thickness change of the plate and it was 5%, 10% or 20%. The cold-worked specimens were respectively designated as SM5, SM10 and SM20, while SM0 denoted the specimen free of cold working. The

tensile properties are shown in Table 1 and they were obtained using specimens taken along the rolling direction. The yield strength for the cold-worked specimens was defined by the 0.2% proof strength.

The stress–strain curves are shown in Figure 1. Although the uniform elongation of SM0 was 14.7%, it was only 2.1% for SM20. Therefore, the stress-strain curves for the cold worked specimens are not sufficient to simulate specimen deformation during SP tests. In the previous study [5], the stress-strain curve of the materials was obtained using the iterative procedure as schematically shown in Figure 2. By using the digital image correlation (DIC) technique, the local strain at the root of the hourglass shaped specimen was measured. Then, the stress-strain curve which reproduced the change in load with the local strain was determined by an iterative FEA. Finally, true stress-strain curves were obtained as shown in Figure 1(b).

Table 1. Mechanical properties of carbon steel (room temperature).

Material	Cold working (%)	Yield Strength (MPa)	Ultimate strength (MPa)	Elongation (%)	Reduction in area (%)	Young's modulus (GPa)
SM0	0	365	534	29.7	74.6	208
SM5	5	494	572	24.0	75.6	209
SM10	10	547	592	19.3	71.6	208
SM20	20	607	640	15.0	69.8	207

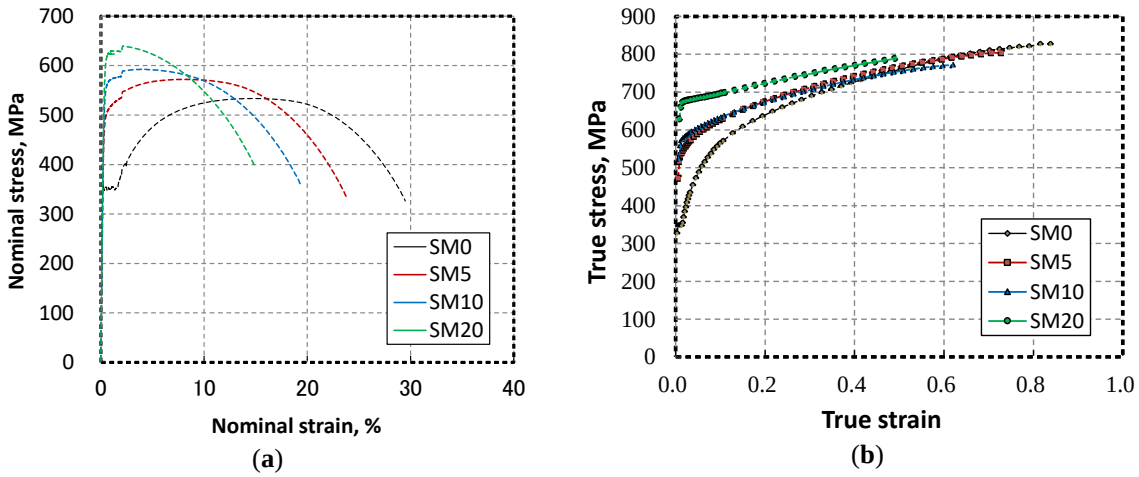

Figure 1. Stress-strain curve of test materials. (a) Nominal stress-strain curve; (b) true stress-strain curve obtained by iterative procedure.

2.2. Test procedure

Disc-type specimens, with a diameter of 8 mm, were used for SP tests. The normal direction of the disc specimen was the same as that of the plate. A single specimen was prepared for SM0, SM5, SM10 and SM20. The thicknesses of the specimen t were 0.4994 mm (SM5), 0.5015 mm (SM20), 0.5041 mm (SM10) and 0.5214 mm (SM0) and the surface was finished using #1200 emery paper.

The specimens were subjected to the SP tests at room temperature using the test device shown in Figure 3. The specimen was fixed by upper and lower dies. The inner diameter of the lower die was 4 mm. No lubrication was applied to reduce friction between the specimen, ball and dies. The ball of 2.3812 mm diameter was indented into the specimen surface at a constant rate of 0.2 mm/m at the cross-head of the tensile test machine.

The displacement was measured using the DIC technique. The lower surface of the specimen was observed by two cameras. In this measurement procedure, the compliance of the test device could be excluded from the displacement measurement.

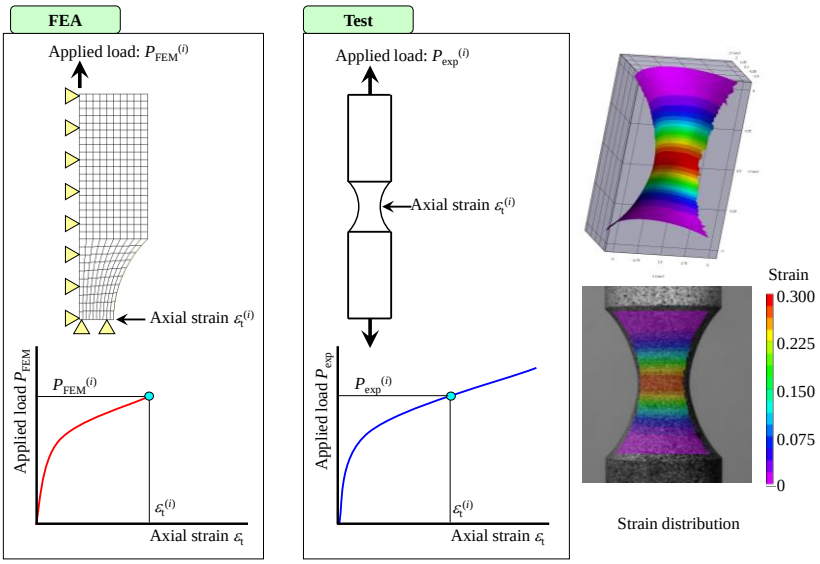

Figure 2. A schematic drawing for the procedure to determine the stress-strain curve using an hourglass shaped tensile specimen (to determine $\sigma_t(i)$ at $\varepsilon_t(i)$).

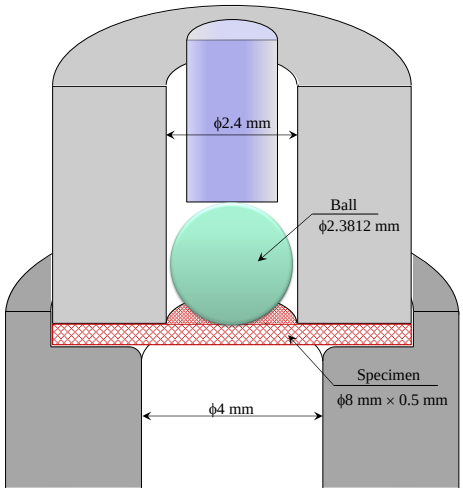

Figure 3. Schematic drawing of SP test device.

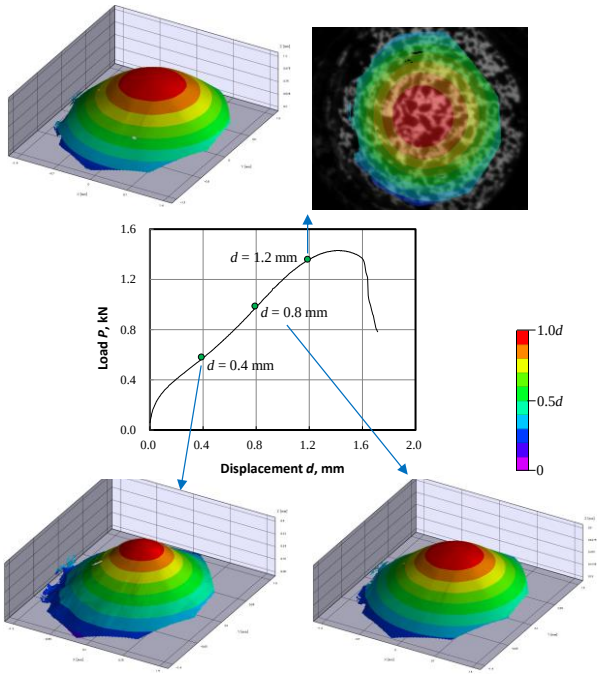

Figure 4. Load displacement curve obtained by the SP test using SM0 specimen. The displacement was measured using the DIC technique.

2.3. Test results

Figure 4 shows the LD curve obtained in the test using the SM0 specimen. The DIC technique could successfully measure the displacement field and the maximum peak of the displacement was quantified as the displacement *d*. The LD curves obtained for each material are shown in Figure 5. The cold working increased the load for the same displacement. Since the SM0 specimen was relatively thick, it showed a relatively large maximum load.

From the LD curve, the yield strength σ_y and ultimate strength σ_u were estimated using the following equations:

$$\sigma_y = \alpha \frac{P_{t/10}}{t^2} \quad (1)$$

$$\sigma_u = \beta \frac{P_{max}}{t \cdot d_{max}} \cdot \quad (2)$$

A line having an inclination that was parallel to the LD curve of the elastic bending region was drawn so that it passed through the point of $d = 0.1t$ at $P = 0$. Then, the load of the cross point of the line and the LD curve was defined as $P_{t/10}$ [1]. The constant $\alpha = 0.364$ was obtained in Ref. [1]. The ultimate strength was estimated using the maximum peak load P_{max} and the displacement at P_{max}, which is noted as d_{max}. It was shown that $\beta = 0.277$ gave a good estimation for various materials [1]. The estimated yield and ultimate strengths were compared with the tensile test results in Figure 6. Although the estimated ultimate strengths agreed well with the tensile test results, the yield strengths exhibited smaller values.

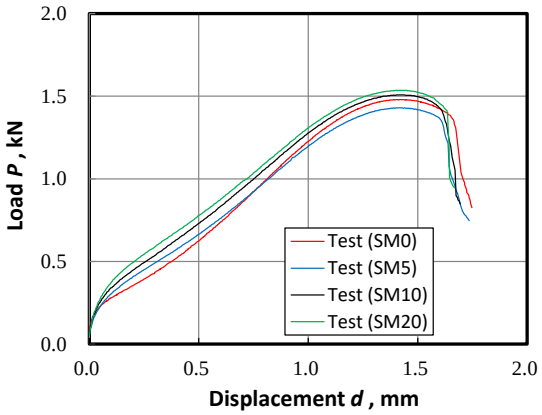

Figure 5. Load displacement curves obtained by the SP tests.

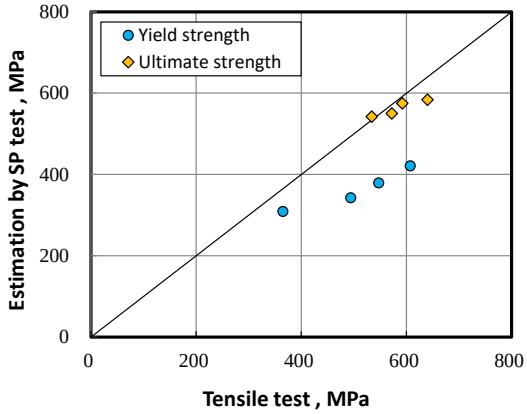

Figure 6. Estimation of the yield and ultimate strengths from load-displacement curves obtained. by the SP tests.

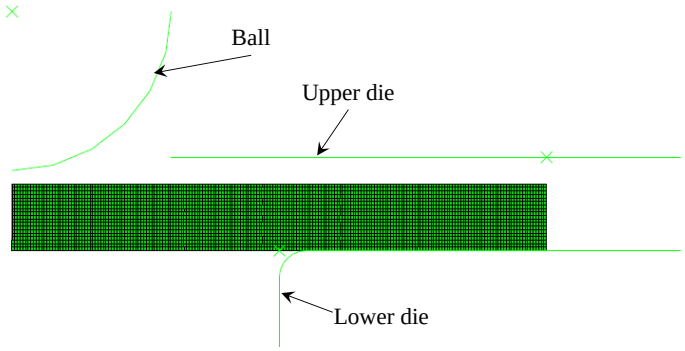

Figure 7. Finite element model for simulating SP tests.

3. Finite element analyses

3.1. Analysis procedure

Isotropic hardening elastic–plastic FEAs were performed using the finite element model shown in Figure 7 together with the stress-strain curves shown in Figure 1(b). The true stress-strain curve was extrapolated to 2.0 in true strain to simulate large deformation. The SP test specimen was modeled with axisymmetric linear reduced integration elements (CAX4R). Due to geometrical symmetries, only one half of the specimen was modeled with the displacement boundary conditions on the plane of symmetry. The upper and lower dies for fixing the specimen and indentation ball was modeled using rigid bodies, which were non-deformable bodies.

First, axial force was applied to the upper die to fix the specimen as done in the test. Then, the ball was moved to press into the specimen. The friction coefficient between the ball and specimen was set to 0.1. ABAQUS standard Version 6.14 was applied as the FEA solver. To simulate large inelastic deformation during the test, the nonlinear geometry option with ABAQUS (the NLGEOM option) was invoked.

3.2. Analysis results

Figure 8 plots LD curves obtained by FEAs together with test results. The FEA simulated well the change in the load with the displacement at the lower surface. Particularly, the result for SM0 specimen was almost identical to the test result. The load of the FEA tended to be larger for the cold-worked specimens, although the maximum load was almost the same as the test results.

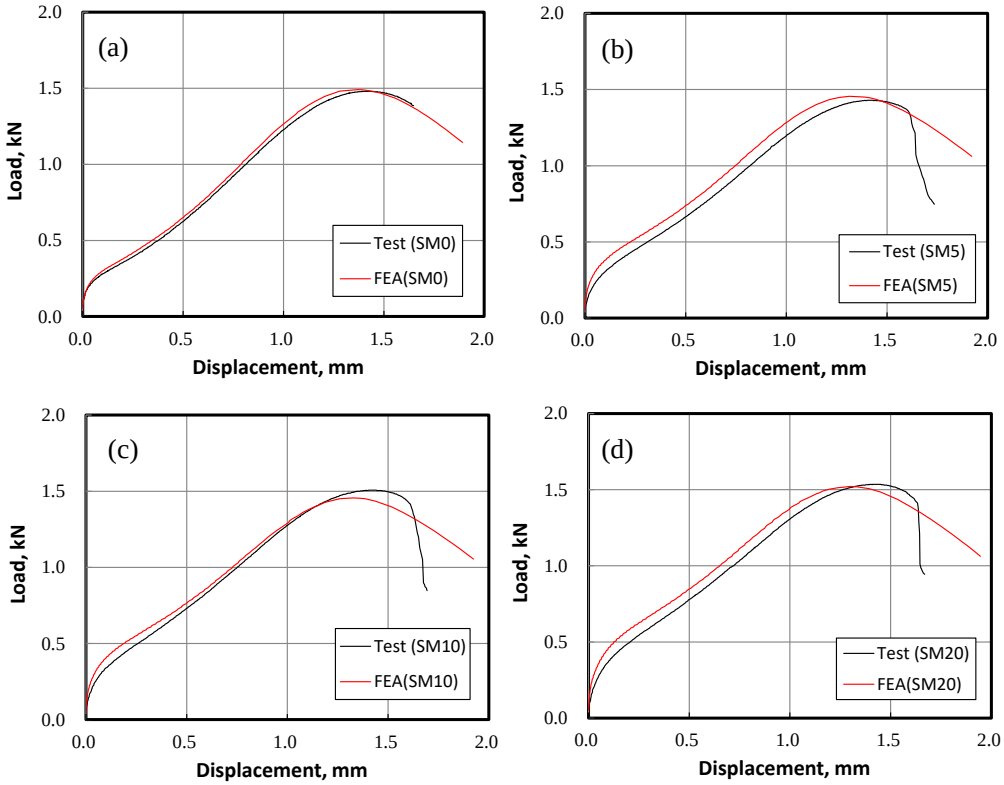

Figure 8. The load-displacement curves simulated by FEAs. (a) SM0; (b) SM5; (c) SM10; (d) SM20.

4. Discussion

4.1. Estimation of ultimate strength

The maximum load P_{max} and the displacement d_{max} were used to estimate the ultimate strength in Equation (2). In order to investigate the correlation between P_{max}, d_{max} and the ultimate strength, FEAs were performed for the various stress-strain curves shown in Figure 9. The curves were modified from that of SM0. The maximum stress of the stress-strain curve used for the previous analysis was sufficiently large, being 1500 MPa corresponding to the true strain of 20. Meanwhile, in Figure 9, it was assumed that the true stresses could not be more than the set values, which were 827, 792, 732 and 649 MPa. It should be noted that these stresses were more than the ultimate strength, which was 612 MPa in the true stress.

Figure 10 shows the LD curves obtained using the stress-strain curves assuming the specimen thickness of t = 0.5 mm. P_{max} and d_{max} were almost the same when the maximum true stress was more than 792 MPa. However, P_{max} and d_{max} decreased apparently when the maximum stress was 732 or 649 MPa, which corresponds to true strain of 0.41 or 0.21, respectively. Since the ultimate strength was 612 MPa, the change in P_{max} and d_{max} was not brought about by the change in the ultimate strength. The peak position seemed to depend not on the ultimate strength as discussed in Kumar et al. [6].

As shown in Figure 6, the ultimate strength can be predicted well by Equation (2) using P_{max} and d_{max}. However, it is just an empirical correlation. It is difficult to say that Equation (2) is valid for a general case.

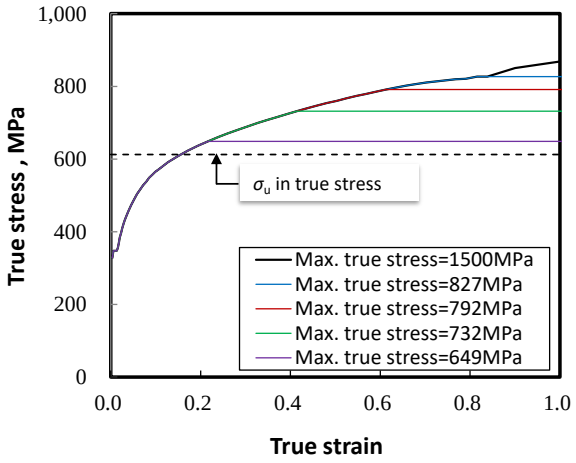

Figure 9. Modeled stress-strain curves used for FEAs. The maximum true stresses were no more than the set values.

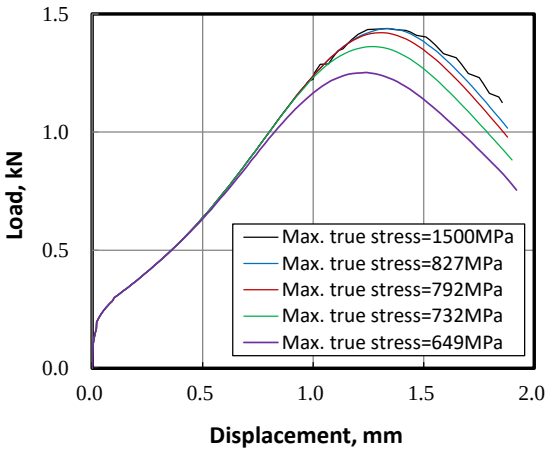

Figure 10. Load-displacement curves obtained using various stress-strain curves (t = 0.5 mm).

4.2. Estimation of yield strength

The yield strength was estimated using $P_{t/10}$ in Equation (1). To investigate the validity of the estimation procedure, the estimation was conducted for the modeled stress-strain curves shown in Figure 11. Simplified bi-linear stress-strain curves were defined using the plastic slopes of E_p = 0, 500, 1000, and 1500 MPa, while the elastic slope (Young's modulus) of 200,000 MPa and yield strength of 200 MPa were assumed to be the same. Figure 12 shows the yield strength estimated by Equation (1) using the LD curve obtained by the simulation. Although the estimated yield strength should be 200 MPa regardless of E_p, it slightly depended on E_p. An almost identical value was obtained when E_p = 1500 MPa, and it was 171 MPa when E_P = 0. Since the change in estimated yield strength was relatively small compared with the wide variation of E_P, it can be concluded that the deflection point in the LD curve correlates well with the yield strength.

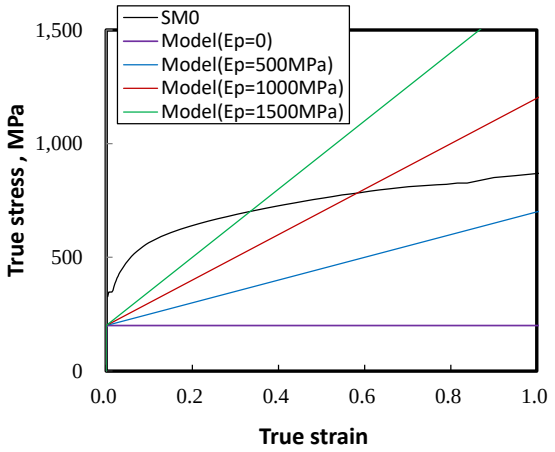

Figure 11. Modeled stress-strain curves used for FEAs.

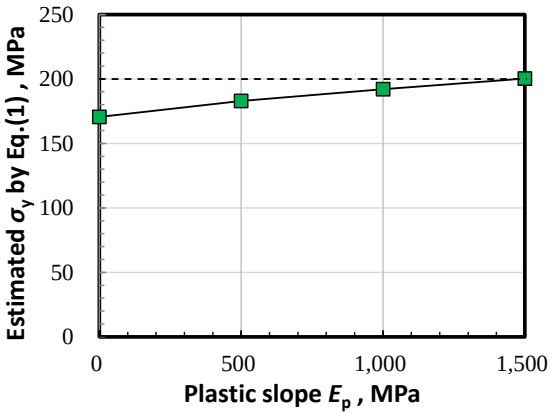

Figure 12. Estimated yield strength obtained using different stress-strain curves (t = 0.5).

The specimen thickness was used to estimate the yield strength in Equation (1). It was pointed out that the use of t^2 was better for correcting influence of the specimen thickness on the estimation. Figure 13 shows the constant α obtained for various stress-strain curves and specimen thicknesses. The value of α was calculated from Equation (1) by substituting the assumed yield strength σ_y and $P_{t/10}$ obtained by the simulation. The obtained α was larger than the value proposed in Ref. [1]. Therefore, the accuracy of the yield strength can be improved by applying a larger α. However, α depends on the specimen thickness.

In order to exclude the influence of the specimen thickness on the yield strength estimation, various definitions of the deflection point in the LD curve were investigated. Finally, it was found that the deflection point of $P_{0.3mm}$ was better than $P_{t/10}$. As shown in Figure 14, the offset displacement of 0.3 mm was quoted for determining $P_{0.3mm}$. Then, the yield strength was estimated by:

$$\sigma_{y(0.3mm)} = \alpha_{0.3mm} \frac{P_{0.3mm}}{t^2}. \quad (3)$$

The constant $\alpha_{0.3mm}$ was obtained by substituting the assumed yield strength into the expression for $\sigma_{y(0.3mm)}$. Figure 15 shows the change in $\alpha_{0.3mm}$ with the specimen thickness. An almost constant $\alpha_{0.3mm}$ was obtained regardless of the specimen thickness. The average value for all data shown in Figure 15 was $\alpha_{0.3mm}$ = 0.229. By performing the simulations for various stress-strain curves, it is possible to determine a better value for the constant $\alpha_{0.3mm}$.

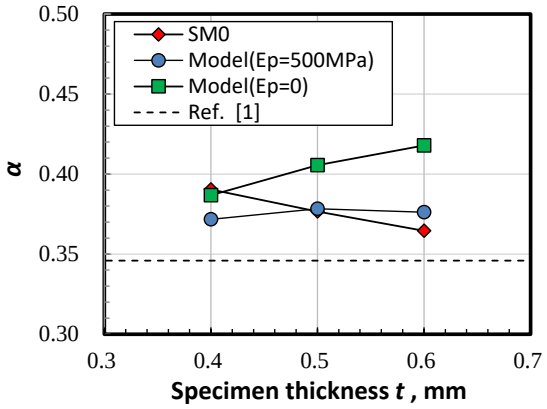

Figure 13. Constant α to estimate the yield strength obtained for various specimen thicknesses and stress-strain curves.

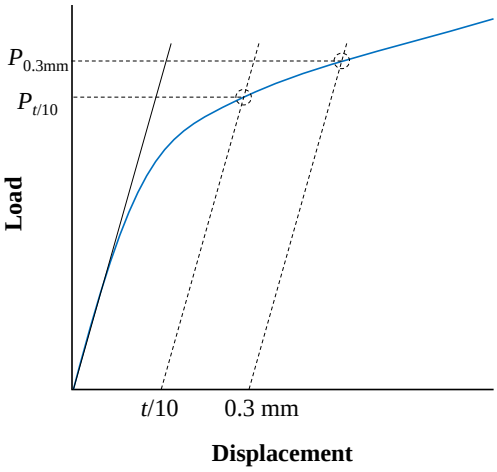

Figure 14. Definition of deflection points $P_{y(t/10)}$ and $P_{y\,(0.3mm)}$.

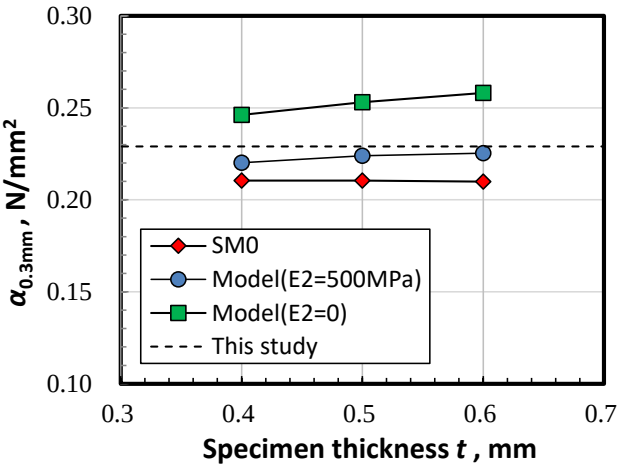

Figure 15. Constant $\alpha_{0.3mm}$ to estimate the yield strength obtained for various specimen thicknesses and stress-strain curves.

5. Conclusions

The SP tests were conducted for carbon steel specimens with and without cold working. The DIC technique was applied to measure the displacement. Then, by using the true stress-strain curves including post-necking strain, detailed FEAs were carried out for the SP tests. The following conclusions were drawn.

- The DIC technique enabled measurement of the specimen displacement free from compliance of the test device.

- Detailed FEAs using the stress-strain curves including the post-necking strain could reproduce the LD curve. Use of the nominal stress-strain curve obtained by the conventional tensile test was not enough to simulate the maximum load P_{max}.
- Although the empirical ultimate strength estimation obtained by Equation (2) worked well for the current material, it was shown that the maximum load P_m and displacement d_{max} quoted in Equation (2) did not have a direct correlation with the ultimate strength.
- The deflection point in the LD curve correlated with the yield strength.
- The yield strength estimated by Equation (1) depended on the specimen thickness. It was shown that the thickness dependency on the yield strength estimation could be excluded by using $P_{0.3mm}$.

References

1. García, T.E.; Rodríguez, C.; Belzunce, F.J.; Suárez, C. Estimation of the mechanical properties of metallic materials by means of the small punch test. *Journal of Alloys and Compounds* 2014, Vol. 582 (2014), pp.708-717.
2. Mao, X.; Takahashi, H. Development of a further-miniaturized specimen of 3 mm diameter for TEM disk (ø 3 mm) small punch tests. *Journal of Nuclear Materials* 1987, Vol.150, pp.42-52.
3. Fleury, E.; Ha, J. S. Small punch tests to estimate the mechanical properties of steels for steam power plant: I. Mechanical strength. *International Journal of Pressure Vessels and Piping* 1908, Vol.75, pp.699-706.
4. Sainte Catherine, C. S.; Messier, J.; Poussard, C.; Rosinski, S.; Foulds, J. Small Punch Test: EPRI-CEA Finite Element Simulation Benchmark and Inverse Method for the Estimation of Elastic Plastic Behavior, Small Specimen Test Techniques: Fourth Volume, ASTM STP 1418, M. A. Sololov, J. D. Landes, and G. E Lucas, Eds., (2002), pp.350-370.
5. Kamaya, M.; Kawakubo, M. A procedure for determining the true stress-strain curve over a large range of strains using digital image correlation and finite element analysis. *Mechanics of Materials* 2011, Vol. 43, pp.243-253.
6. Kumar, K.; Pooleery, A.; Madhusoodanan, K.; Singh, R. N.; Chakravartty, J. K.; Shriwastaw, R. S.; Dutta, B. K.; Sinha R. K. Evaluation of ultimate tensile strength using miniature disk bend test. *Journal of Nuclear Materials* 2015, Vol.461, pp.100-111.